

Design of hybrid forward boost converter for renewable energy powered electric vehicle charging applications

ISSN 1755-4535
 Received on 1st February 2019
 Revised 30th March 2019
 Accepted on 8th April 2019
 E-First on 6th June 2019
 doi: 10.1049/iet-pe.2019.0151
 www.ietdl.org

Peter K. Joseph¹, Elangovan Devaraj¹ ✉

¹School of Electrical Engineering, Vellore Institute of Technology, Vellore, Tamilnadu, India

✉ E-mail: elangovan.devaraj@vit.ac.in

Abstract: The grid-connected electric vehicle charging stations are being integrated into renewable energy for preserving the conventional energy resources as well as to ensure sustainable development of the society. In addition to the effortless charging, the sudden demand variations in the grid can be met by the renewable energy storage system in the charging stations. The main challenge in this concept is the unstable nature of renewable energy. As the energy storage system of charging station is directly connected to the renewable energy source like a solar panel, according to the variable and deficient input power condition, the converter should supply a regulated output at the required magnitude. If a conventional converter is used for this purpose, the charging efficiency will be poor for higher gain conditions. This article presents a hybrid forward-boost converter to overcome this challenge. By maintaining the power transfer efficiency higher, the gain can be varied to supply a regulated voltage, even for very low input conditions in this proposed topology. The maximum overall efficiency of 95% is achieved for a variable input condition of 30–50 V to provide an output voltage of 170 V. The concept is validated by implementing a 150 W hybrid converter.

Nomenclature

D	duty cycle of switch
EV	electric vehicle
f	switching frequency of converter
N_P	primary number of turns of transformer
N_S	secondary number of turns of transformer
V_{in}	converter input voltage
V_O	converter output voltage
V_P	primary voltage of transformer
V_S	secondary voltage of transformer

1 Introduction

The twenty-first century has witnessed a plethora of revolutionary events in the transportation sector. Electrification of the vehicle stands in the first position among them. For the charging of these electric vehicles, charging stations were established throughout the globe. The ultimate objective of vehicle electrification is to achieve emission-free transportation. Since the electricity generation in most of the developing countries is from thermal power plants, the conventional grid-powered electric vehicle (EV) charging stations cannot claim pollution-free transportation [1, 2]. The only advantage of such EV system is that it can converge the pollution to a smaller area like power plants and the mitigation methods can be applied there.

To overcome this situation, the renewable energy integrated EV charging stations were introduced [3, 4] to the EV sector. The initial implementations were based on grid-renewable hybrid charging stations [5]. Here, the grid will supply energy to the EV in the case of deficient renewable power. The advantage is that no additional storage system is required in this case. Apart from that, the surplus energy provided by renewable sources can be fed back to the grid for power factor correction [6]. As a technical advancement, stand-alone renewable energy powered charging stations were introduced into the transportation sector [7–10]. In stand-alone renewable energy powered charging stations, the entire power requirement will be met by renewable energy. The surplus energy will be stored in a storage battery. For meeting the demand in renewable energy deficient conditions, an energy storage battery is used here along with the former system. To charge this battery

directly from renewable energy sources, some challenges have to be faced.

The renewable energy supply is always flexible due to its weather dependency. For solar-based energy generation, according to the solar irradiation, the output voltage varies. For higher radiation, it will provide higher or optimum output. For shaded or cloudy conditions, it will provide minimum output. Similarly for wind-based renewable energy generation, as per the availability of wind, the output voltage of the harvesting system varies. As the converter is taking input from the renewable energy source directly, the voltage regulation and required amplification should be provided by the converter circuit itself. For medium power EV charging applications, the DC–DC converter circuit should amplify the input voltage to a higher value [11–14]. Several topologies [15–18] were suggested for this application. In the case of higher input variation, the charging efficiency is reducing rapidly in conventional topologies for ensuring the regulated output, especially during very low input conditions.

To mitigate this research gap in conventional topologies, a hybrid converter is proposed here. As the conventional converters and hybrid converters for renewable energy powered EV charging applications are concentrating on providing the regulated output voltage for charging the EV battery [11–18], the overall loss and voltage stress are inclining rapidly for minimum voltage conditions. The solution is to design different converters for these different conditions. The advantages of one converter should overcome the disadvantages of others. With a proper hybrid integration of different converters, this goal can be achieved. The proposed converter can ensure higher efficiency, even for very low input voltage for supplying a regulated output voltage simultaneously. The design, hardware implementation, and result analysis are discussed in the following sessions.

2 Conventional converters

In the selected application, the renewable energy source giving a variable output in the range of 30–50 V. For the battery charging, a nominal voltage of 170 V is required. As the input voltage is very less compared to the required output voltage, a voltage step-up action is inevitable. Different types of DC to DC step-up converters available, each having their own merits and demerits. The real

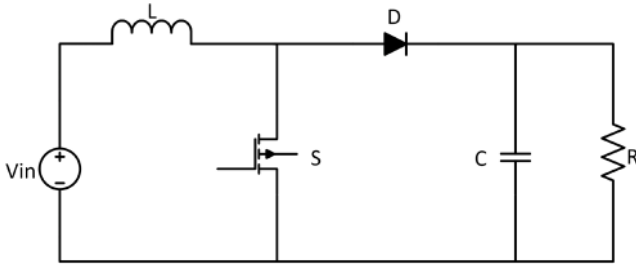


Fig. 1 Circuit diagram of a boost converter

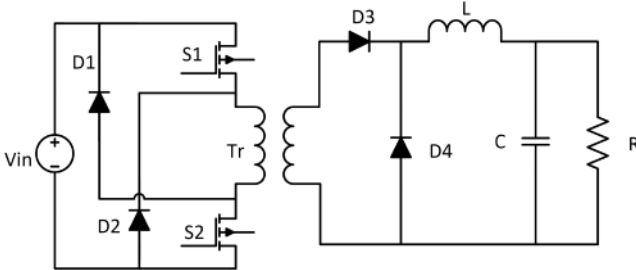


Fig. 2 Circuit diagram of a forward converter

challenge is a high order of variation in the input. At maximum input voltage conditions, a normal gain boost converter can be used. For minimum input voltage conditions, a high gain converter needs to be selected without affecting the conversion efficiency. As per these requirements, two conventional converters are chosen as a boost converter for the first case and a forward converter for the second case.

2.1 Boost converter

The boost converter is a fundamental non-isolated type step-up converter. For medium and lower duty conditions, high conversion efficiency can be achieved with a gain less than unity. For higher input conditions, the boost converter can be used in the battery charger circuit in charging station. The main elements of a boost converter are an inductor, capacitor, switch, diode, and load.

Fig. 1 shows the circuit diagram of a boost converter. When the switch is ON, the input inductor L will get charged and it is discharged along with the input supply voltage when the switch is open [4]. The stored energy in the input inductor during ON state of the switch can be defined as

$$V_{in} = V_L = L \times \frac{\Delta i_L}{\Delta T_{on}} \quad (1)$$

V_{in} and V_L are the input and inductor voltages and Δi_L and ΔT_{on} are the change in current and time during the turn-on time, respectively. The gain of the converter is given by the equation

$$V_{out} = \frac{V_{in}}{1-D} \quad (2)$$

D is the duty of the converter. The advantages of the boost converter are the simplicity of the circuit, high efficiency with low or medium duty cycle etc. A disadvantage of the boost converter is the possibility of a short circuit at a higher duty cycle. The converter efficiency is less at higher duties.

2.2 Forward converter

The forward converter is a type of isolated type converter. As forward converter can provide a gain more than unity without any considerable decrease in efficiency, it can be used for lower input operating conditions. The main components include four diodes, two switches, one transformer, one inductor, one capacitor, and a load.

Fig. 2 illustrates the circuit diagram of a forward converter. During the ON condition of S_1 and S_2 , the input voltage (V_{in})

appears across the primary (V_p) of transformer Tr. Then, the secondary voltage can be defined as

$$V_S = V_P \times \left(\frac{N_S}{N_P}\right) \quad (3)$$

where N_S and N_P are the primary and secondary number of turns of the transformer. Now the inductor voltage can be found using KVL from Fig. 2 as

$$V_L = V_S - V_O = V_{in} \times \left(\frac{N_S}{N_P}\right) - V_O = L \times \frac{\Delta i_L}{\Delta t} \quad (4)$$

When the primary switches are in off condition, diodes D_1 and D_2 will be conducting. Now, the secondary voltage V_S in (3) will be changed to

$$V_S = V_P \times \left(\frac{N_S}{N_P}\right) = -V_{in} \times \left(\frac{N_S}{N_P}\right) \quad (5)$$

Since D_3 is not conducting and D_4 is conducting, the voltage across the inductor, V_L becomes

$$V_L = -V_O = L \times \frac{\Delta i_L}{\Delta t} \quad (6)$$

From the steady-state analysis, the gain of the forward converter can be found as

$$V_O = D \times V_{in} \times \left(\frac{N_S}{N_P}\right) \quad (7)$$

The main advantage of the forward converter is that the gains above and below unity can be achieved by just varying duty and turns ratio. Adding more number of turns to get more output voltage will reduce the efficiency of the system due to elevated winding copper losses. In addition, it may lead to the saturation of the transformer core. Since both of the mentioned converter techniques having the desired advantages and considerable disadvantages as per their operating mode, a combination of both may result in an optimised topology.

3 Proposed hybrid converter

Since forward converter can provide step-up action in low input voltage conditions with high efficiency as well as boost converter can provide the step-up actions during medium and high input voltage conditions, a hybrid step-up converter can be designed by combining the advantages of both converters for a wide input range operation. There are different varieties of converters are available [15–18] other than this two, though by considering various parameters like the number of components, compactness, transfer efficiency, voltage stress over switch and gain factor, these two are the best options for designing a hybrid converter in this context. While designing a hybrid converter, various challenges have to be considered. While integrating one converter with another, there should not be a performance conflict between the converters. Simultaneously, the individuality should be maintained as well as the disadvantages should be mitigated. A design circuit diagram is shown in Fig. 3.

The proposed converter consists of a controllable switch S_1 , one mechanical switch S_2 , four capacitors, two inductors, four diodes, and one transformer. The function of a mechanical switch is to jump from boost converter mode to forward converter mode or vice versa. There are two operating modes for this hybrid converter according to the status of mechanical switch S_2 .

3.1 Mode 1 (S_2 is closed)

In mode 1 operation, S_2 is closed and the circuit exhibits the property of a forward converter. The detailed current flow diagram of mode 1 is illustrated in Fig. 4. Mode 1 can be again divided into

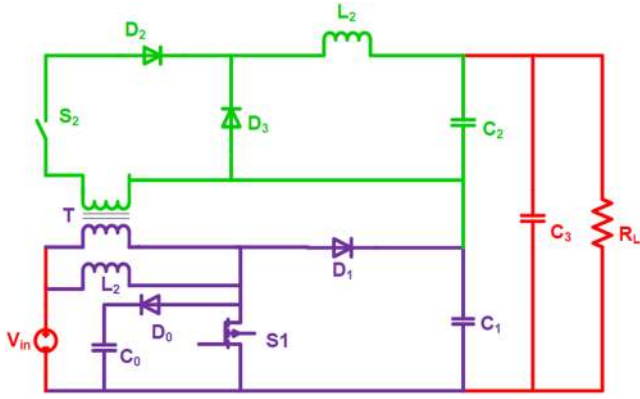


Fig. 3 Proposed hybrid converter circuit

four sub-modes accordingly, depending on S_1 status and current flow direction through C_2 . The operation in mode 1 is illustrated in Fig. 4.

When S_1 is closed as in Fig. 4a, the value of inductor current can be found as

$$V_p = V_{in} = L_1 \frac{\Delta i_{L_1}}{\Delta T_{on}} \quad (8)$$

$$\Delta i_{L_1} = \frac{\Delta T_{on} V_{in}}{L_1}$$

Considering Fig. 4b, the flow and rate of change of current through L_2 can be derived from the voltage across L_2

$$V_{L_2} = \left(V_{C_1} - V_{in} \times \frac{N_S}{N_P} \right) - V_O = L_2 \times \frac{\Delta i_{L_2}}{\Delta T_{on}} \quad (9)$$

$$\Delta i_{L_2} = \frac{\left(V_{C_1} - V_{in} \times \frac{N_S}{N_P} \right) - V_O}{L_2} \times \Delta T_{on}$$

By applying the KVL in this condition, diode voltages V_{D_1} and V_{D_3} can be found out. D_1 and C_1 will come in parallel with same voltage. Similarly, transformer secondary voltage will come across diode D_3 .

$$V_{D_1} = V_{C_1} \quad (10)$$

$$V_{D_3} = V_S = V_{in} \frac{N_S}{N_P}$$

The second stage of mode 1 starts, when S_1 is opened. Now V_p and V_S can be found from

$$V_p = V_{in} - V_{C_1} \quad (11)$$

$$V_S = (V_{in} - V_{C_1}) \times \frac{N_S}{N_P}$$

By analysing the current flow directions in Figs. 4c and d, the voltage and current flow rate through L_2 can be derived as

$$V_L = -V_{C_2} = L_2 \times \frac{\Delta i_{L_2}}{\Delta T_{off}} \quad (12)$$

$$\Delta i_{L_2} = \frac{-\Delta T_{off} V_{C_2}}{L_2}$$

For modelling the steady-state equation, the cumulative sum of rate of change of current flow through L_2 should be zero. So add (9) and (12).

$$\frac{\left(V_{C_1} - V_{in} \times \frac{N_S}{N_P} \right) - V_O}{L_2} \times \Delta T_{on} - \frac{\Delta T_{off} V_{C_2}}{L_2} = 0 \quad (13)$$

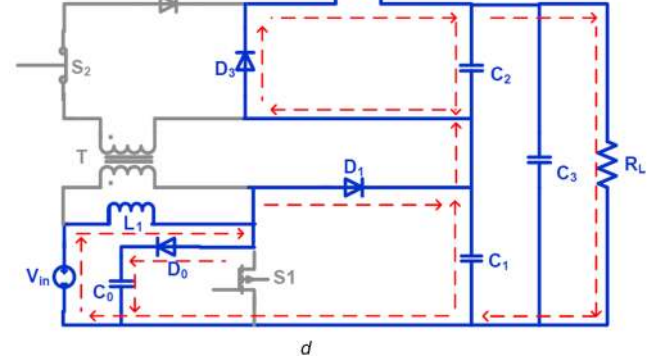
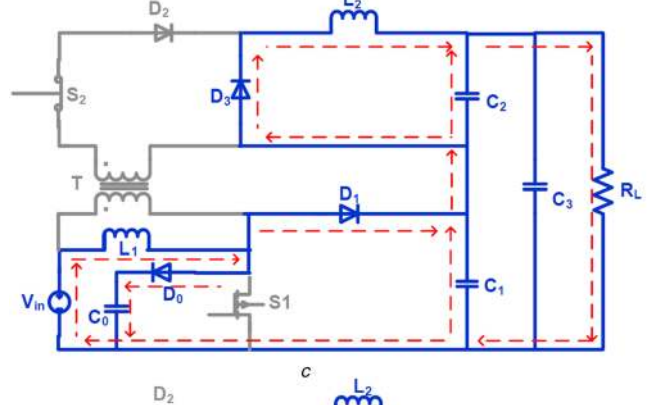
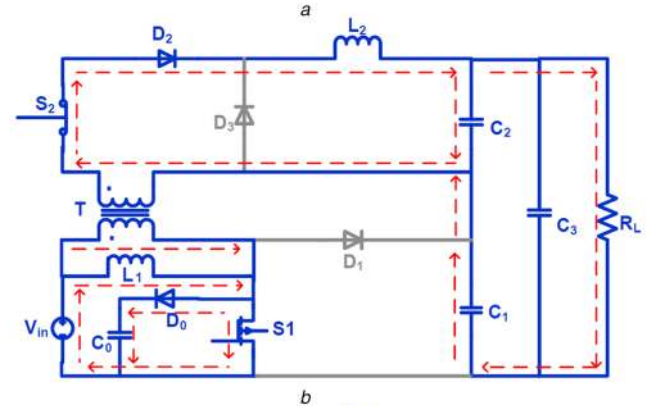
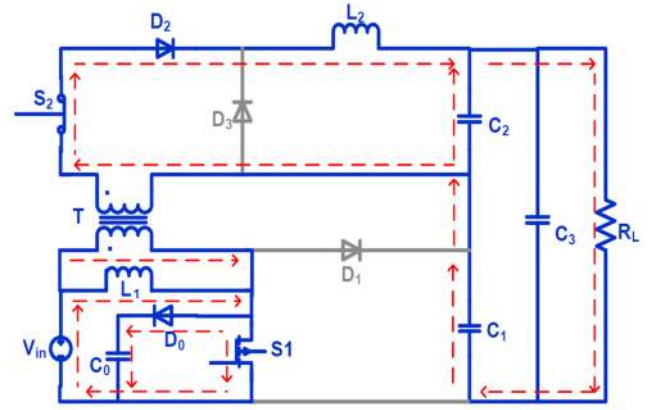


Fig. 4 Mode 1 operation

(a) S_1 is ON, positive current flow in C_2 , (b) S_1 is ON, negative current flow in C_2 , (c) S_1 is OFF, positive current flow in C_2 , (d) S_1 is OFF, negative current flow in C_2

Equation (13) can be modified using the duty ratio analogy. With the duty ratio analogy, the overall gain of the converter can be formed.

$$-V_{C_2}(1 - D) + \left(V_{C_1} + V_{in} \frac{N_S}{N_P} \right) D + V_O D = 0 \quad (14)$$

By applying KVL at the secondary side, V_{C_2} can be obtained as

$$V_{C_2} = V_O - V_{C_1} \quad (15)$$

Substituting (15) in (14), the succeeding equations can be obtained.

$$-(V_O - V_{C_1})(1 - D) + \left(V_{C_1} + V_{in} \frac{N_S}{N_P} \right) D + V_O D = 0 \quad (16)$$

$$V_O = V_{in} \frac{N_S}{N_P} + V_{C_1}$$

Since the output performance of C_2 is like a boost converter, the voltage equation can be implied in the form of a fundamental gain equation of boost converter.

$$V_{C_1} = \frac{V_{in}}{1 - D} \quad (17)$$

By comparing (16) and (17) the gain equation of proposed hybrid converter can be formed.

$$V_O = V_{in} \times \left(D \frac{N_S}{N_P} + \frac{1}{1 - D} \right) \quad (18)$$

So the gain of the proposed hybrid converter only depends on turns ratio and duty in mode 1 operation. After getting the gain equation of mode 2 operation, the overall gain of the proposed converter can be formed.

3.2 Mode 2 (S_2 is open)

In mode 2 operation, S_2 is opened and the circuit performs like a boost converter as the input voltage is relatively high. Now the duty of switches can be chosen as less compared to mode 1 as explained in the previous sessions. As a result, the voltage stress over the switches will be minimum. The detailed current flow diagram of mode 2 is illustrated in Fig. 5. Mode 2 can be again divided into four sub-modes accordingly, depending on S_1 status and current flow direction through C_2 .

When S_2 is opened, no current will flow through D_2 , which indicates that the transformer primary current is magnetising current. In addition, DC current flow through D_3 in the boost converter half of proposed circuit. As D_3 conducts, the current through L_2 will be constant, which causes the voltage across C_2 is zero. So output voltage is equal to V_{C_1} .

To find V_{C_1} , transformer primary analysis is need to be done. When S_1 is conducting, the voltage across L_1 can be found from Figs. 5a and b as

$$V_{L_1} = V_{in} = L_1 \frac{\Delta i_{L_1}}{\Delta T_{on}} \quad (19)$$

$$\Delta i_{L_1} = \frac{\Delta T_{on} V_{in}}{L_1}$$

When S_1 is at off position as illustrated in Figs. 5c and d, only magnetising current will flows through transformer primary.

$$V_{L_1} = V_{in} - V_{C_1} = L_1 \frac{\Delta i_{L_1}}{\Delta T_{off}} \quad (20)$$

$$\Delta i_{L_1} = \frac{(V_{in} - V_{C_1}) \Delta T_{off}}{L_1}$$

For modelling the steady-state equation, the cumulative sum of rate of change of current flow through L_2 should be zero. So add (19) and (20).

$$\frac{\Delta T_{on} V_{in}}{L_1} + \frac{(V_{in} - V_{C_1}) \Delta T_{off}}{L_1} = 0 \quad (21)$$

Equation (21) can be modified using the duty ratio analogy for getting V_{C_1} . The duty ratio analogy can be used to derive the overall gain equation of the proposed system.

$$V_{C_1} = \frac{V_{in}}{1 - D} \quad (22)$$

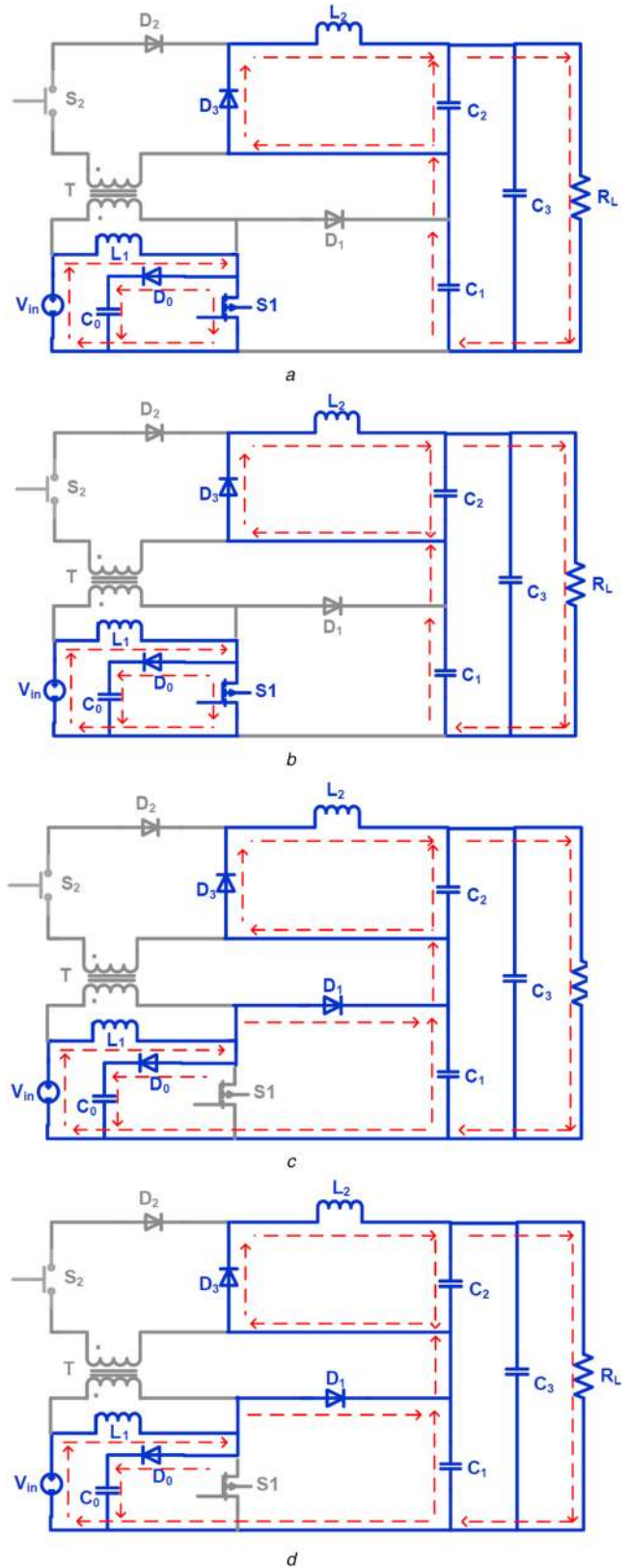


Fig. 5 Mode 2 operation

(a) S_1 is ON, positive current flow in C_2 , (b) S_1 is ON, negative current flow in C_2 , (c) S_1 is OFF, positive current flow in C_2 , (d) S_1 is OFF, negative current flow in C_2

As mentioned earlier, the output voltage is same as V_{C_1} . So the final gain equation of mode 2 will be

$$V_O = \frac{V_{in}}{1-D} \quad (23)$$

With these performance equations of Mode 1 and Mode 2, the converter can be designed and implemented accurately.

4 Design of proposed converter for EV charging

The aim is to design a converter for EV (low power) charging capable providing 200 W, 170 V at the output from a variable input of 30–50 V. Turns ratio of the transformer is selected as 3 from [10].

$$\frac{N_S}{N_P} = 3 \quad (24)$$

To implement the proposed hybrid converter, the inductor values should be more than the minimum required value. The value of inductor L_1 can be derived from the boost converter, which depends on switching frequency (f), duty (D_1) and load resistance (R_L).

$$L_{1min} = \frac{D_1(1-D_1)^2 R_L}{2f} \quad (25)$$

Substituting values as $f = 100$ kHz, $D_1 = 0.7$ and $R_L = 145 \Omega$ in (25), L_{1min} is obtained as 45.67 μ H. Similarly L_{2min} can be derived from the forward converter as

$$L_{2min} = \left[V_{in} \left(\frac{N_S}{N_P} \right) - V_{C_2} \right] \times \frac{D_2}{f \Delta i_{L_2}} \quad (26)$$

D_2 is the duty of forward converter. By substituting the values as $D_2 = 0.6$, $V_{in} = 50$ V, $V_{C_2} = 85$ V, $(N_S/N_P) = 3$, $\Delta i_{L_2} = 4$ A and $f = 100$ kHz in (26), L_{2min} is obtained as 98 μ H. C_{1min} can be derived from the boost converter by considering the ripple percentage (ripple %) as

$$C_{1min} = \frac{D_1}{f \times R_L \times \text{ripple \%}} \quad (27)$$

Considering a 5% of ripple, the C_{1min} is obtained as 1 μ F from (27). Similarly, C_{2min} can be derived from the forward converter as

$$C_{2min} = \frac{1-D_2}{8 \times L_2 \times f^2 \times \text{ripple \%}} \quad (28)$$

By substituting a 5% ripple and 150 μ H L_2 , the C_{2min} is obtained as 1 μ F.

5 Hardware and testing

As per the designed values of the proposed hybrid converter, a hardware setup is implemented to analyse the performance. Fig. 6 illustrates the test setup for the performance evaluation of the proposed converter. Instead of the EV charging station, an equivalent lamp load is connected to test the feasibility. Input is taken from a programmable power supply to simulate the renewable energy input condition. The switching pulses are given by dSPACE controller and a TLP 350 driver board.

By varying the input voltage from 30 to 50 V and controlling the mechanical switch, the performance is evaluated with the setup shown in Fig. 6. As per the input variation, the hybrid converter gives the required output with a precise transition between operating modes.

Fig. 7 shows the implemented hybrid converter circuit. The specifications of the components and parameters used for hardware implementation are enlisted in Table 1. As per the concept derived,

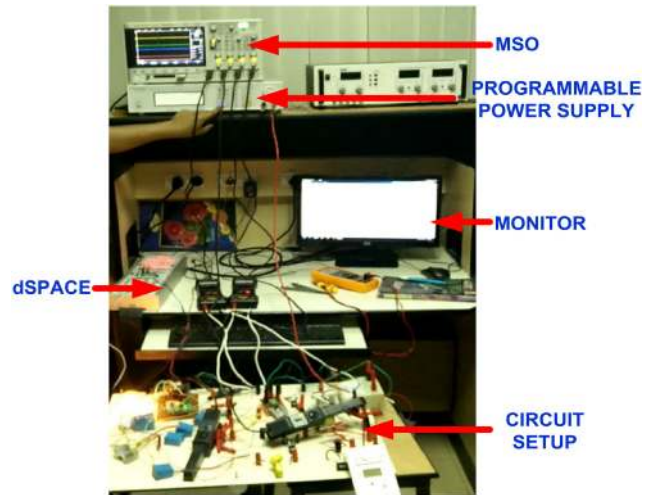


Fig. 6 Hardware test setup

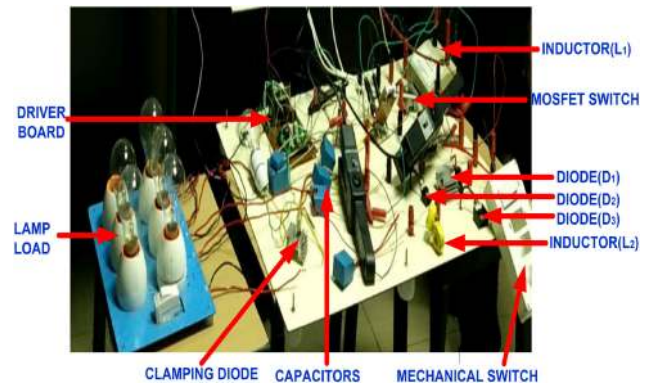


Fig. 7 Proposed hybrid converter

Table 1 Hardware specification

Hardware parameters	Specifications
input voltage (V_{in})	30–50 V
output voltage (V_O)	170 V
output power (P_O)	148 W
load resistance (R_L)	145 Ω
duty ratio (D_1)	0.6
duty ratio (D_2)	0.7
inductance (L_1)	50 μ H
inductance (L_2)	100 μ H
capacitance (C_1)	1 μ F
capacitance (C_2)	1 μ F
capacitance (C_3)	20 μ F
capacitance (C_O)	1 μ F
transformer turns ratio	1:3
switching frequency (f)	100 kHz
MOSFET	IRF640N

if the source voltage is above the designed input voltage of boost converter, then the hybrid mode will be OFF. If the source voltage is less than that, then the hybrid-mode will be ON. Thus, the overall efficiency will be maintained high. The advantages of both converters brought together to obtain a precise and accurate output.

The switching frequency of the proposed system is selected as 100 kHz so that the magnetic size including transformers and inductors can be reduced. In the programmable DC source, a random set of the voltage-current combination was uploaded with the voltage value varies from 30 to 50 V, to realise the instability of renewable power sources. The execution time also set in the

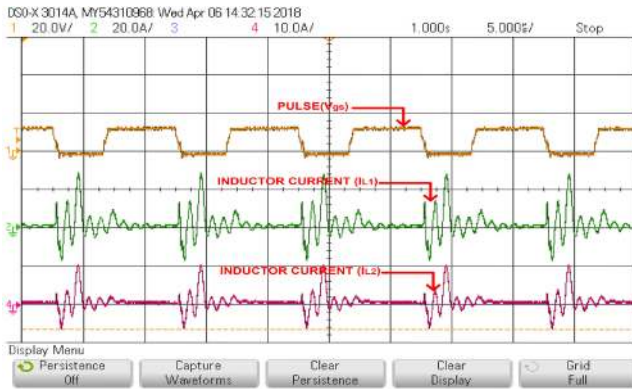


Fig. 8 Inductor currents of L_1 and L_2

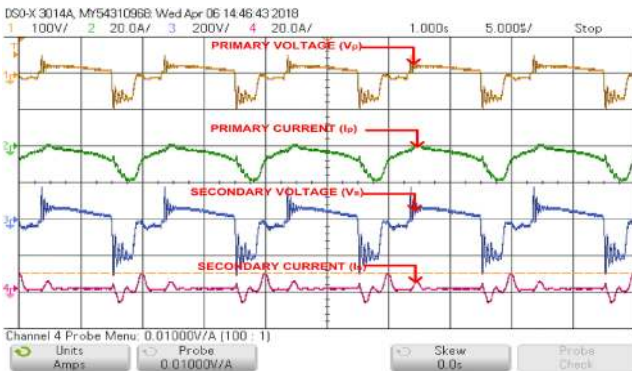
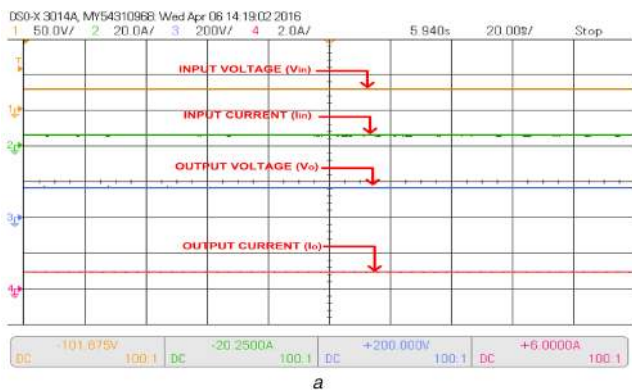
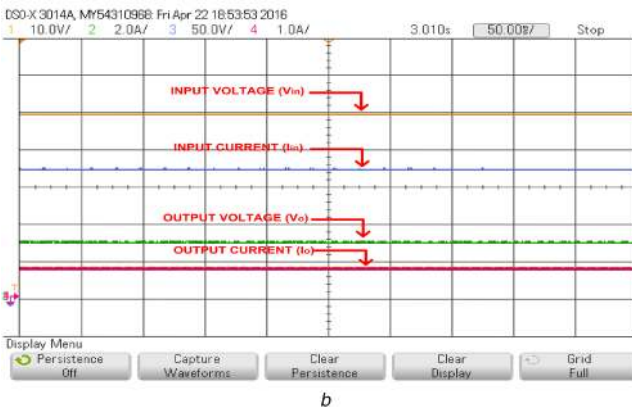


Fig. 9 Transformer waveforms: brown-primary voltage; green-primary current; blue-secondary voltage; pink-secondary current



a



b

Fig. 10 Modes of operation
(a) Hybrid mode, (b) Boost mode

programmable power supply, in order to make a real-time simulation of instability. Since the minimum input voltage is 30 V, the converter is operated in hybrid mode initially. IRF640N MOSFET has a maximum drain-to-source voltage of 200 V and maximum drain current capacity of 18 A, which is matching with

the converter performance in simulation. A reduced drain to source resistance of 0.15Ω will help to reduce the conduction losses of the switch. The maximum duty of the proposed hybrid converter is 0.7, which will protect the switches from voltage stress as discussed in the previous session.

Fig. 8 illustrates the current flowing through the inductors L_1 and L_2 , respectively, in hybrid mode condition along with the switching pulses generated from dSPACE microcontroller. As it is illustrated, the pulses are oscillating at a switching frequency of 100 kHz. The same ripple frequency is visible on the inductor currents of L_1 and L_2 . The ripple current is coming in selected percentage, yet it can be improved by choosing a higher inductor value. As the inductor size increases, the ohmic loss of the system increases. In addition, the system will be bulky. The performance also can be improved by choosing a higher grade driver IC, which is more suitable for higher frequency operating conditions. With the proper selection of an output capacitor, the load can be protected from ripples.

Fig. 9 shows the voltage and current waveforms in the transformer during hybrid mode condition. Compared to Fig. 8, the voltage and current ripples are minimal across the transformer primary and secondary due to optimised design and less effect of source and load dynamics. Secondary current is relatively linear due to the current flow through L_2 and C_2 in Mode 1 as illustrated in Fig. 4.

Fig. 10 illustrates the comparison of hybrid mode and boost mode performance. Though minute ripples are present in the output voltage and output current, the presence of output capacitors helps the proposed hybrid converter circuit to achieve steady DC output waveforms. Fig. 10a represents the hybrid mode operation. Here, mechanical switch is closed as the input is 30 V. An overall efficiency of 90% is achieved in this condition. Fig. 10b represents the boost mode, where the mechanical switch is open corresponding to 50 V input. For both cases, the output voltage is satisfying the required output voltage criteria of 170 V. Overall efficiency of 95.4% achieved in this mode.

Fig. 11 illustrates the performance of the hybrid converter with varying input from 30 to 50 V. The performance is tested for different duty conditions. Duty is varied from 0.4 to 1. A maximum efficiency characteristic is associated with the designed duty cycle of 0.7. The efficiency is decreasing for the duty values which is above and below the duty = 0.7.

Fig. 12 shows the performance comparison of conventional forward and boost converter with the proposed hybrid converter. In the selected range, the hybrid converter exhibits maximum efficiency condition. Compared to all other hybrid converters proposed for renewable energy powered EV charging applications [15–18], the proposed topology is exhibiting high efficiency for providing the rated voltage for the battery. After the testing of the proposed converter, various advantages can be formulated over conventional converters. Compared to a boost converter and forward converter, the proposed topology is having high overall efficiency throughout the operation. To get the required output voltage, conventional converters are having limitation due to voltage stress over switches for a higher duty. The issue is solved up to an extent in this topology. The proposed topology will provide a regulated output for a higher input voltage variation interval, unlike conventional converters. As the required duty and gain are relatively less for the switches in the proposed hybrid converter, the switching stress is very less. According to the levels of input voltages, the operating mode changes in proposed topology, so that an optimum gain can be followed throughout the operation.

Few disadvantages are also associated with the proposed converter. As the proposed converter is formed by combining the features of conventional boost and forward converter, the number of components are high in it, which contributes to the size of the converter. As a mechanical switch is required for the transition from one mode to another according to the input voltage variations, the wear and tear loss will be more for it. Presence of multiple inductors and higher frequency contributes more ripples to the current waveform. As the design depends on the multiple operating modes, input voltage variations, and multiple passive elements, the

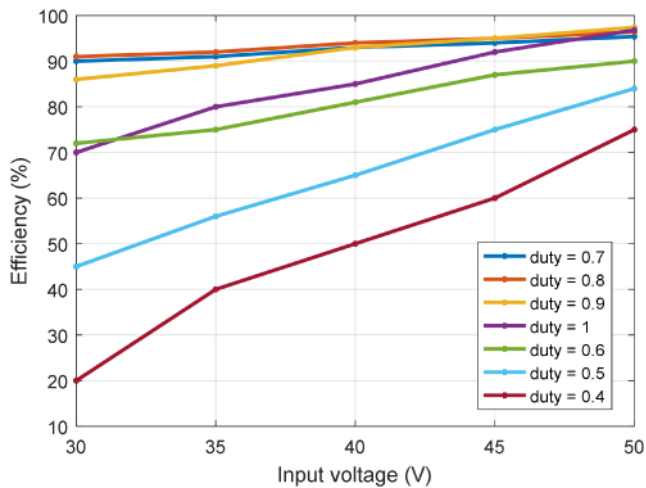


Fig. 11 Performance of hybrid converter

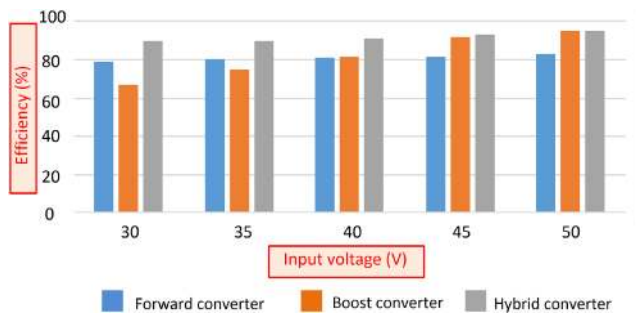


Fig. 12 Performance comparison

system design is relatively complicated. As the switching losses and winding losses are increasing drastically for the higher power range, the performance of the proposed design is not promising for the same.

By considering the overall performance of the proposed hybrid converter, it is the best option for medium power EV charging applications. As a regulated voltage is maintained at the output, irrespective of the wide range input variations with an optimised efficiency, the proposed hybrid converter is perfectly suitable for stand-alone renewable energy powered charging stations for electric vehicles.

6 Conclusion

Grid-connected charging stations for electric vehicles are being replaced by stand-alone renewable energy powered charging stations due to grid power quality effects and the abundant supply of renewable energy. In stand-alone charging stations, the surplus energy needs to be stored into a battery for renewable source deficient conditions. Since renewable sources are highly dynamic due to nature dependency, the design of the battery charging circuit is a riddle for researchers. As the input voltage is varying for a wide range, the use of conventional converters will result in higher voltage stress over switches and reduced transfer efficiency. To mitigate the dispute, a plethora of converter designs were evolved,

yet the conversion range – converter gain dilemma sustained well. As a key to the quest, this paper presents a simple boost-forward hybrid converter for an input voltage range of 30–50 V. Using the forward converter principle in low input values and boost converter principle in higher input values, the input variation range problem is tackled. The maximum overall efficiency of 95.4% is achieved in this range for a 148 W hybrid converter model.

7 Acknowledgments

This research work is funded by 'VIT SEED GRANT', 2018.

8 References

- [1] Leithon, J., Lim, T.J., Sun, S.: 'Cost-aware renewable energy management with application in cellular networks', *IEEE Trans. Green Commun. Netw.*, 2018, **2**, (1), pp. 316–326
- [2] Sun, J., Li, M., Zhang, Z., *et al.*: 'Renewable energy transmission by HVDC across the continent: system challenges and opportunities', *CSEE J. Power Energy Syst.*, 2017, **3**, (4), pp. 353–364
- [3] Luo, C., Huang, Y.F., Gupta, V.: 'Stochastic dynamic pricing for EV charging stations with renewable integration and energy storage', *IEEE Trans. Smart Grid*, 2018, **9**, (2), pp. 1494–1505
- [4] Mohan, V., Singh, J.G., Ongsakul, W.: 'Sortino ratio based portfolio optimization considering EVs and renewable energy in microgrid power market', *IEEE Trans. Sustain. Energy*, 2017, **8**, (1), pp. 219–229
- [5] Chen, Q., Wang, F., Hodge, B.M., *et al.*: 'Dynamic price vector formation model-based automatic demand response strategy for PV-assisted EV charging stations', *IEEE Trans. Smart Grid*, 2017, **8**, (6), pp. 2903–2915
- [6] Chaudhari, K., Ukil, A., Kumar, K.N., *et al.*: 'Hybrid optimization for economic deployment of ESS in PV-integrated EV charging stations', *IEEE Trans. Ind. Inf.*, 2018, **14**, (1), pp. 106–116
- [7] Pareek, A., Singh, P., Rao, P.N.: 'Analysis and comparison of charging time between battery and supercapacitor for 300 W stand-alone PV system'. Int. Conf. on Current Trends Towards Converging Technologies (ICCTCT), Tamilnadu, India, 2018, pp. 1–6
- [8] Feng, R., Xu, J., Wu, G.: 'Research on joint coordination control of stand-alone wind-solar systems with battery storage'. China Int. Conf. on Electricity Distribution (CICED), Tianjin, People's Republic of China, 2016, pp. 1–6
- [9] Amanor-Boadu, J., Sanchez-Sinencio, E., Asmah, M.W.: 'A universal fast battery charging and management solution for stand-alone solar photovoltaic home systems in sub-saharan Africa'. IEEE PES PowerAfrica, Accra, Ghana, 2017, pp. 174–179
- [10] Zhou, B., Xu, D., Li, C., *et al.*: 'Optimal scheduling of biogas-solar-wind renewable portfolio for multicarrier energy supplies', *IEEE Trans. Power Syst.*, 2018, **33**, (6), pp. 6229–6239
- [11] Bhattacharyya, K., Mandal, P.: 'Technique for the reduction of output voltage ripple of switched capacitor-based DC-DC converters', *IET Circuits Devices Syst.*, 2011, **5**, (6), pp. 442–450
- [12] Lin, B.R., Zhang, S.Z.: 'Analysis and implementation of a three-level hybrid DC-DC converter with the balanced capacitor voltages', *IET Power Electron.*, 2016, **9**, (3), pp. 457–465
- [13] Engelkemeir, F., Gattozzi, A., Hallock, G., *et al.*: 'An improved topology for high power soft-switched power converters', *Int. J. Electr. Power Energy Syst.*, 2019, **104**, pp. 575–582
- [14] Ray, O., Mishra, S.: 'Boost-derived hybrid converter with simultaneous DC and AC outputs', *IEEE Trans. Ind. Appl.*, 2014, **50**, (2), pp. 1082–1093
- [15] Monteiro, V., Ferreira, J.C., Melendez, A.A.N., *et al.*: 'Experimental validation of a novel architecture based on a dual-stage converter for off-board fast battery chargers of electric vehicles', *IEEE Trans. Veh. Technol.*, 2018, **67**, (2), pp. 1000–1011
- [16] Taylor, A., Lu, J., Zhu, L., *et al.*: 'Comparison of SiC MOSFET-based and GaN HEMT-based high-efficiency high-power-density 7.2 kW EV battery chargers', *IET Power Electron.*, 2018, **11**, (11), pp. 1849–1857
- [17] Zhang, Y., Gao, Y., Zhou, L., *et al.*: 'A switched-capacitor bidirectional DC-DC converter with wide voltage gain range for electric vehicles with hybrid energy sources', *IEEE Trans. Power Electron.*, 2018, **33**, (11), pp. 9459–9469
- [18] Restrepo, M., Morris, J., Kazerani, M., *et al.*: 'Modeling and testing of a bidirectional smart charger for distribution system EV integration', *IEEE Trans. Smart Grid*, 2018, **9**, (1), pp. 152–162